CHAPTER-V

CHAPTER - V

STUDIES OF CdS AND CdS:Sb BASED PHOTOELECTROCHEMICAL (PEC) CELLS

5.1 Introduction :

Now a days thin films of chalcogenide semiconductors found worldwide applications in various fields of science and technology including solar cells. Solar cells are considered to be one of the possible alternatives to the depleting resources of energy such as fossil fuels, coal etc. It is the prohibitive cost of single crystal solar cells that has turned the interest of scientific community to the possibility of using the semiconducting thin films which are prepared by either the chemical or the physical methods. Wastage of material, high cost per surface area of deposition, instability, deposition temperature and tedius and typical instrumentation are few of the many disadvantages of all the physical methods. On the other hand, simple ease of preparation, minimum active materials, low cost per area of deposition and doping capabilities are distinct superiorities of the chemical methods. The semiconductors which possess an appropriate energy bandgap seems to be effective in photovoltaic energy conversion. Being an intermidiate bandgap, semiconductor direct mode of transition, high coefficient of absorption, and stability against photodissolution; Cadmium sulphide is a promising material in this context. Solar Cells can be made by the solid-solid junctions and also by the semiconductor-liquid junction, the later has certain overriding advantages, such as junction formation by merely immersing the thin films in a suitable electrolyte, minimization of a lattice mismatch, thermal expansion problems and a wide choice and control

over the redox potential in solution state. Since the photovoltaic properties are the direct consequences of the material properties, the choice lies both for the preparation and characterization techniques for a material.

The literature data shows a large number of preparative methods for the deposition of cadmium sulphide both in single crystal and polycrystalline forms, [25-30, 43, 94-100]. The optical to electrical energy conversion efficiency uptill reported is quite below the expectation and is generally supposed to be due to its higher resistivity. Considering all the facts into accounts, we have planned to deposit the doped and undoped cadmium sulphide thin films by our modified chemical deposition process and employed them to form a photoelectrochemical cells.

Section 5.2 describes the design fabrication of a PEC cell and the experiemntal procedure for some measurements on photoelectrochemical cells. These experimental observations have been discussed in section 5.3.

5.2 Experimental Details :

The samples, both CdS and CdS:Sb deposited onto stainless steel substrates were utilised for the construction of a photoelectrochemical cell. The experimental conditions mentioned earlier were adopted while depositing the samples (Chapter III).

5.2.1 Design and fabrication of a photoelectrochemical (PEC) cell:

To start with it was essential to fabricate a suitable cell of the suitable dimensions. The cell used in this investigations was fabricated in our laboratory and is shown in fig. 5.1(a,b).

It consists of two test tubes, one hard glass test tube of the inner diameter 2.7 cm and length 7 cm. approximately, and other ordinary test tubes of the inner diameter 1.5 cm and length 12 cm. The tubes were connected by means of a capillary whose diameter equals approximately 0.5 cm. This H-shaped assembly was fitted in a copper pot of a suitable size. A window of dimensions 2 x 0.5 cm was made for illumination of the photoelectrode.

The PEC cell was constructed by employing the CdS and CdS:Sb samples as a photoelectrode, a mixture of 1M NaOH-1M Na_2S -1M S as an electrolyte and a sensitised graphite rod as a counter electrode. The distance between a photoelectrode and a counter electrode was of the order of 0.3 cm. A rubber cork was used for air tightening of the cell and to support the counter and photoelectrodes. The active area of the sample was defined by a common epoxy resin. The sensitisation of a counter electrode was subjected to CoS treatment before use in PEC cell.

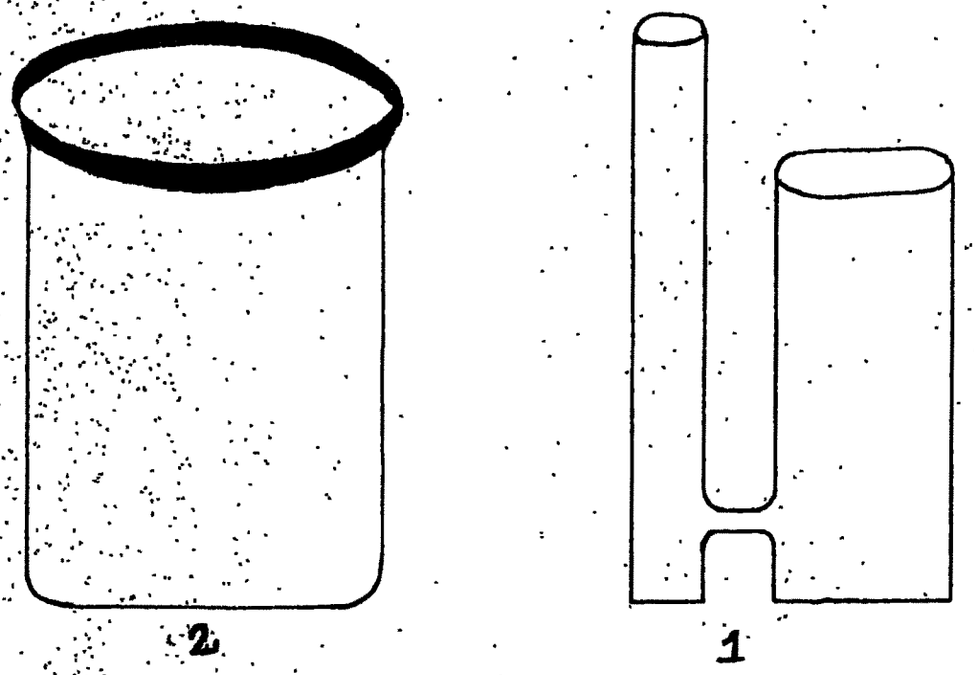

Fig. 5.1(a) Design constituents of a Cell : (1) Glass Cell
(2) Copper Pot

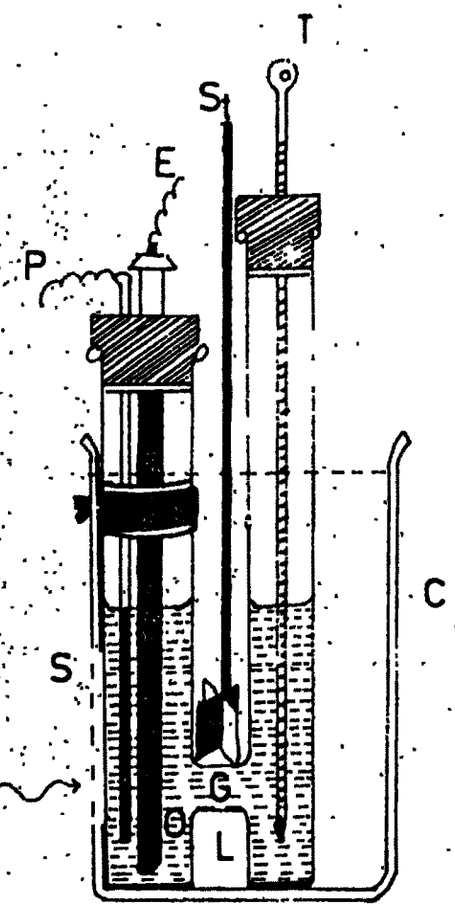

Fig.5.1 (b) Fabrication of a PEC cell showing :
P - Photoelectrode
E - Counter electrode
G - Glass Cell
C - Copper pot
S - Slit
St - Stirrer
L - Liquid electrolyte.
T - Thermometer

5.2.2 Measurements on PEC cell :

The various measurement techniques employed in order to characterise PEC cell are as under :

a) Nature of contact between CdS/CdS:Sb and substrate :

The nature of contact between the CdS material and stainless steel was examined. The sample on substrate was mounted between two copper press contacts. One contact was pressed on stainless steel (film on this end was removed) while other was pressed directly on the film. Press contacts were made tight by a screw arrangement. An experimental arrangement for this is more or less similar to the conductivity measuring unit. A variable potential was applied across the sample and current for each applied potential was measured as described earlier. The necessary care was taken for the insulation between the sample and the conducting surfaces of the unit.

b) Electrical and optical studies on a PEC cell :

Design and contructional details of a PEC cell are outlined in section 5.2.1. The electrical properties of the PEC cell can tell us about the charge transfer process across the electrode-electrolyte interface. In view of this, current-voltage characteristic in dark, power output curve, photo, and spectral responses were studied. This section gives the informations about the

experiemntal arrangements for both electrical and optical studies of the PEC cells.

i) Experimental for electrical properties :

The circuitry as shown in fig. 5.2 was used to study both I-V and C-V measurments. The applied junction potential was varied with a 10 turn 1KΩ potentiometer and was noted with a Agronic, 3 1/2 digit, voltmeter. The current flowing through the junction was noted with a HIL 2665, - 4 1/2 digit current meter. The cell was illuminated through a window by means of a 250W bulb and care was taken against heating of the cell (water filter was interposed between the lamp and a cell). The C-V measurement was carried out (vs.SCE) under reverse biasing of the junction by using the same circuit as above. The differential capacitance was measured by a Aplab-4910. Capacitance meter at a superimposed 1KHz frequency and an a.c. voltage of 1 volt peak to peak.

ii) Experiemental for optical properties :

The measurements of a short circuit current and open circuit voltage for different intensities of illumination were carried out. The illumination was measured with a digital lux meter LX-101 (Lutron, Taiwan). The spectral response of a cell was recorded by using a

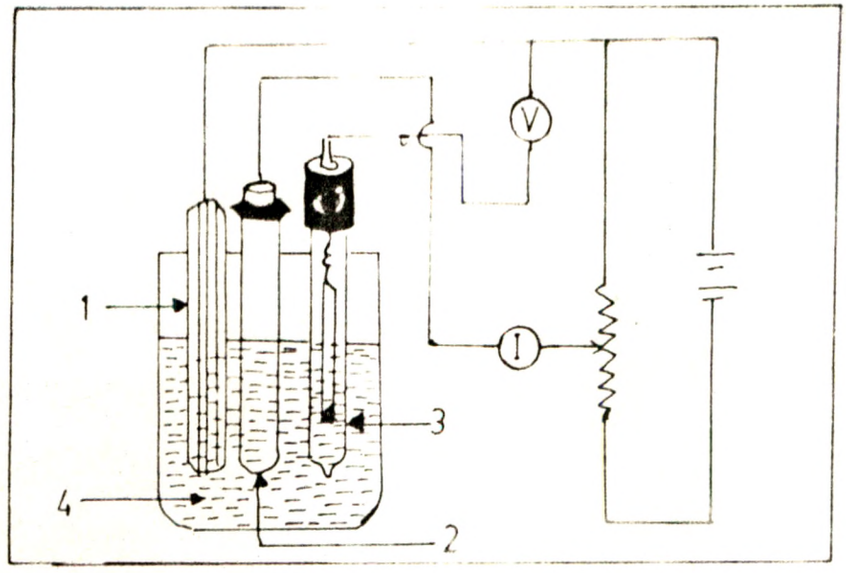

Fig. 5.2 : An experimental arrangement for electrical characterisation of a PEC Cell :
1) Photoelectrode, (2) Counter electrode,
3) Saturated Calomel Electrode (SCE) (4) Electrolyte

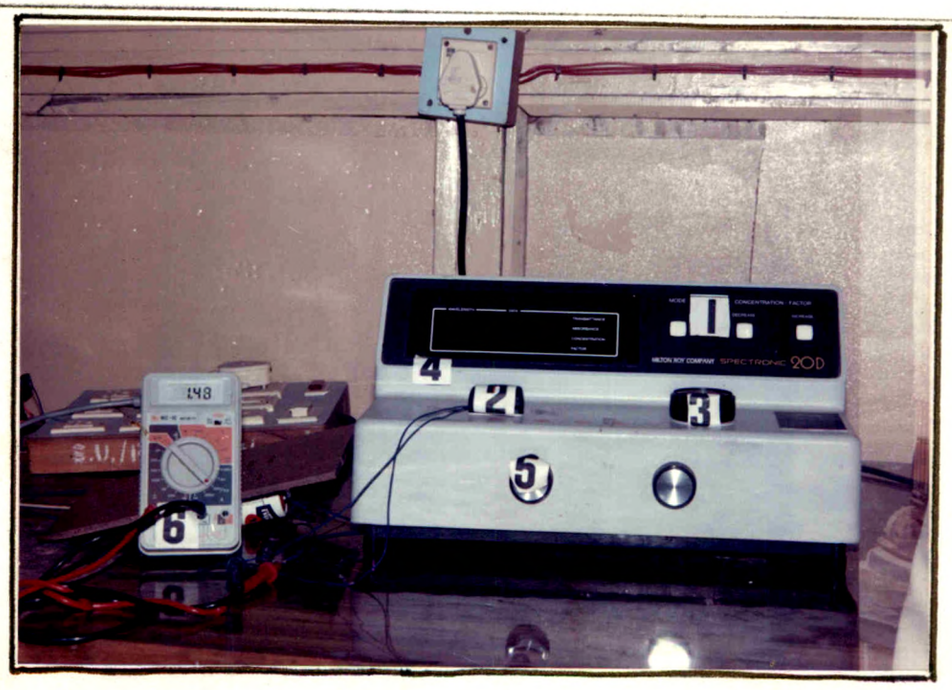

Fig. 5.3 : Photograph of the experimental setup for spectral response of a PEC Cell :
1) Spectrophotometer (2) PEC cell (3) Wavelength Monitor
4) Wavelength (nm), (5) Set zero and ON/OFF
6) Current meter.

spectro photometer (digispectronic, 20 D, Milton and ROY, USA) in the wavelength range 400 nm to 1000 nm.

A photograph of an experimental set up is shown in fig.5.3.

5.3 Results and Discussion :

The studies so far available in the literature show that the exposure of a n-CdS photoelectrode to an electrolyte solution drastically decreases the performance of a PEC cell. These studies coupled with some other experimental observations made us clear that the method of preparation for the material will not yield satisfactory results in a reproduciable fashion. Apparently crystallites of certain dimensions are necessary for the preparation of photoactive electrodes. The X-ray diffraction and optical microscopy have shown that the films of n-CdS prepared by various techniques consist of small crystallites which are not sufficient to absorbe all the incident photons. Thus it is proper to say that the grain size should be large enough compared with optical absorption deth [105]. Therefore in this work we have used polycrystalline CdS thin film as one of the active electrodes to form a photoelectrochemical cell.

As the nature of contact between the substrate and the material plays an important role in determining the efficiency of conversion, the nature of contact between

CdS/CdS:Sb and stainless steel was tested as explained in the previous section. For an efficient performance of a PEC device the contact between the film photoelectode and the substrate should be ohmic. A contact is said to be ohmic, if it is non-injecting and has a linear I-V relation in both directions [106]. In practice a contact is assumed to be ohmic, if voltage drop across it in either direction is negligible compared to that across the device, and hence does not perturb significantly the device performance. Actually the linearity of contact I-V relationship is therefore not important if the voltage is small. The nature of contact between CdS and stainless steel was examined. The equilibrium current potential relation, pertaining to the nature of contact is found to be linear and symmetric for both types of polarity. This suggests that the work function of CdS/CdS:Sb is greater than that of the contact material [8, 45,93,95,107]. The bands bend downward at the surface, and an accumulation region which is a reservior of majority carriers is formed. The contact offers a little resistance to the flow of current through the semiconductor material for the moderate applied voltage of either polarity.

In our case the contact resistance is of the order of a few ohms. The equilibrium I-V characteristic for the contact between CdS/CdS:Sb and stainless steel is shown in fig. 5.4.

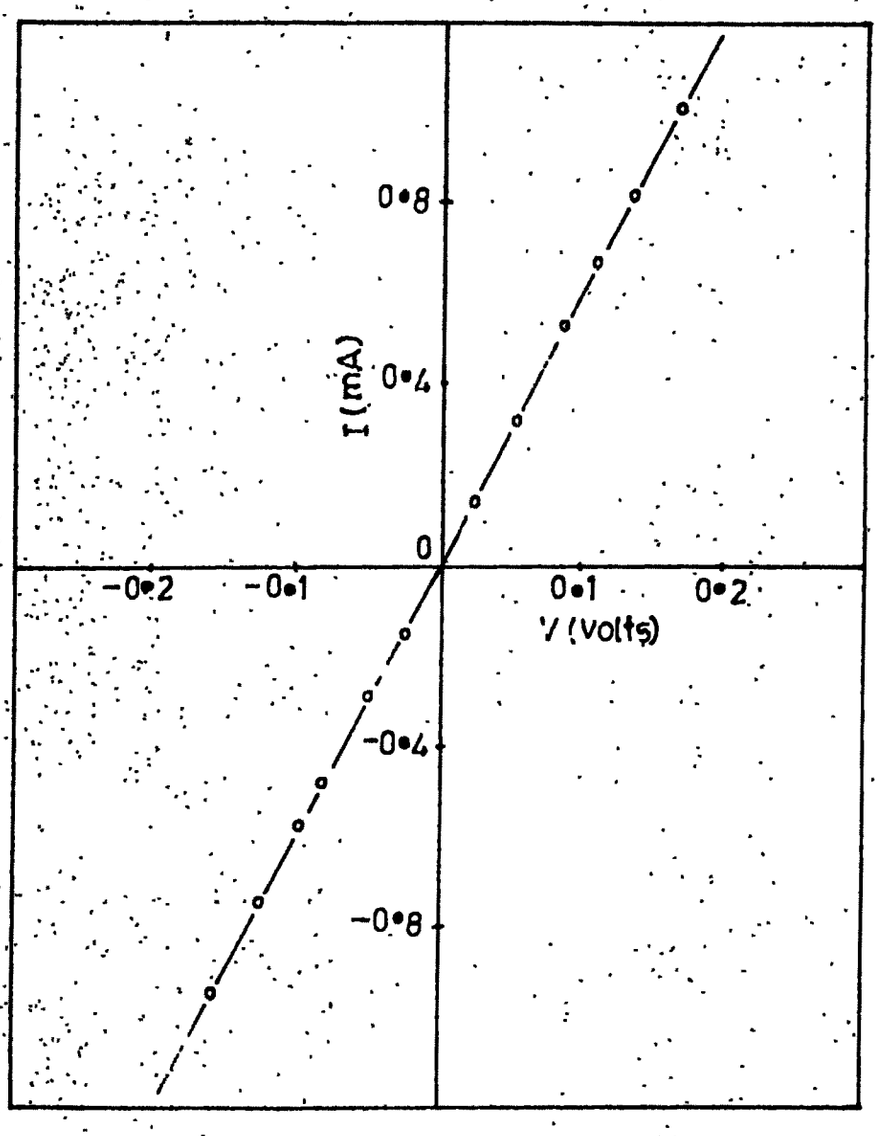

Fig. 5.4 : Nature of contact between CdS/CdS:Sb and stainless steel.

5.3.1 Electrical Properties :

An electrolyte/semiconductor interface properties namely, current voltage characteristic in dark, capacitance voltage characteristic in dark, and current voltage characteristic under lighted condition have been considered in this section.

a) Current voltage characteristics in dark :

The current voltage characteristics in dark of the PEC cells consisting of CdS and CdS:Sb active photoelectrodes havae been studied. It is seen that the voltagae called as the dark voltage, V_D, and current called as the dark current, I_D, are generated in all the cells. The polarity of dark voltage is negative towards CdS/CdS:Sb photoelectrode and positive towards the counter electrode. The origin of dark voltage can be ascribed to the difference in two half cell potentials in a PEC cell which are related as [95].

$$E = E_{n\text{-}CdS/CdS:Sb} - E_{carbon} \quad \ldots (5.1)$$

where $E_{n\text{-}CdS/CdS:Sb}$ and E_{carbon} are the half cell potentials developed when CdS/CdS:Sb photoelectotrode and carbon counter electrode are immersed into an electrolyte. From the observed polarity of the voltage it is seen that:

$$E_{n\text{-}CdS/CdS:Sb} < E_{carbon} \quad \ldots (5.2)$$

The existence of a dark current, I_D, in a cell suggests that there is some deterioration of the active photoelectrode material in dark. In order to understand

the charge transfer process across the semiconductor/electrolyte interface, the dynamic I-V curves have been further analysed. It has been that forward current increases rapidly with the applied bias voltage. The increase in forward current is due to a small contact barrier height and an increase in possible tunneling mechanism [108,109]. The current in reverse bias condition does not saturate but increases with an applied voltage. Following are possible reasons [108] : i) The effective barrier height (ϕ_b) decreases, because of the interfacial layer ii) Electron-hole pairs are thermally generated in the depletion region of the semiconductor under high reverse bias condition, and iii) The current increases due to the onset of an electron injection from the electrolyte into the semiconductor because the barrier becomes thin enough for tunneling to take place. The nature of the I-V curve can be explained on the basis of the nature of the charge transfer mechanism defined by a Butler-Volmer relation as [60].

$$I = I_o\left[\exp(1-\beta)\frac{V\cdot F}{RT} - \exp\left(-\frac{\beta V\cdot F}{RT}\right)\right] \quad \ldots\ldots (5.3)$$

Where, I_o is the equilibrium exchange current density, β is the symmetry factor, V is the over voltage, R is the universal gas constant and F is the Faraday constant, and T is the absolute temperature.

When $\beta = 0.5$, eqn (5.3) becomes :

$$I = I_o\left[\exp\left(\frac{V\cdot F}{2RT}\right) - \exp\left(\frac{-VF}{2RT}\right)\right] \quad \ldots(5.4)$$

and is further expressed as :

$$I = 2I_o \sinh\left(\frac{F \cdot V}{2RT}\right) \qquad \ldots(5.5)$$

The I vs sinh V curve is symmetrical and a symmetry factor of 0.5 corresponding to a symmetrical barrier yields a symmetrical I vs V curves. This means that interface cannot rectify a periodically varying potential and/or current.

If $\beta \neq 0.5$ then I Vs V currve would not be symmetrical and the interface has rectifying properties called as Faradaic rectification [60]. The nonsymmetrical nature of the I-V curve in the forward and reverse bias configurations show that the junction formed in all these PEC cells is rectifying and is analogous to a Schottky barrier junction. The values of junction qualify factor in dark (n_d), for all the cell configurations are evaluated from the log I vs V variation in response to a schottky diode equation for the semiconductor electrolyte interface. The variation of log I vs V is a straight line and is shown in fig. 5.5 for four typical cells. The magnitude of n_d can be determined from high voltage region of this plot. The values of n_d lies in the range from 2.17 to 2.72. It is seen that all the values of dark quality factor are greater than unity which indicates that the junctions are non-ideal. The deviation of n_d from unity suggests that the dark I-V characteristics are often influenced by recombination mechanism and series resistance effects

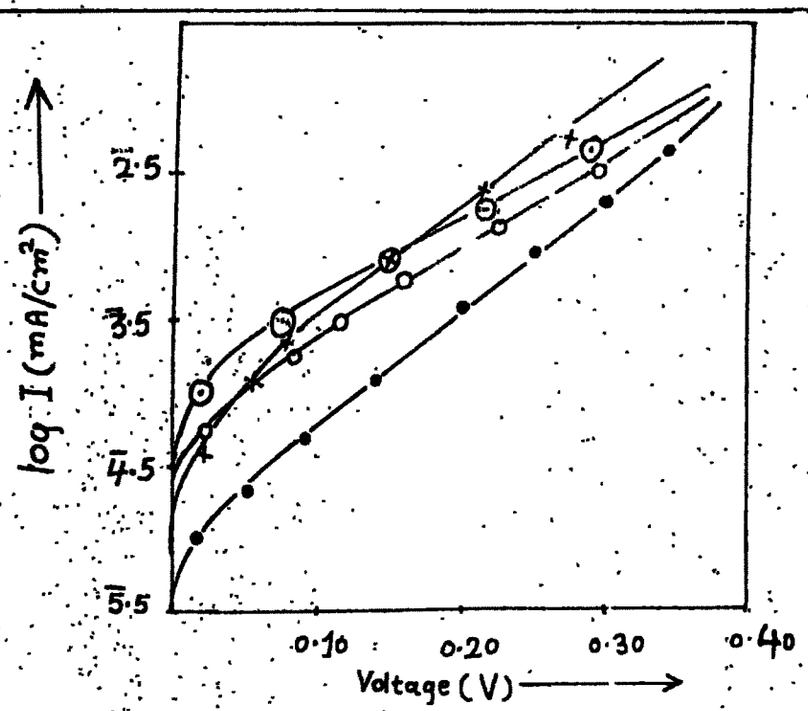

Fig. 5.5 : Variation of log I vs. V for the cells formed with different photoelectrodes :
1] ⊙ - pure CdS (2) O - 0.005 wt% CdS:Sb
3) ● - 0.075 wt% CdS:Sb and (4) x - 0.25 wt% CdS:Sb

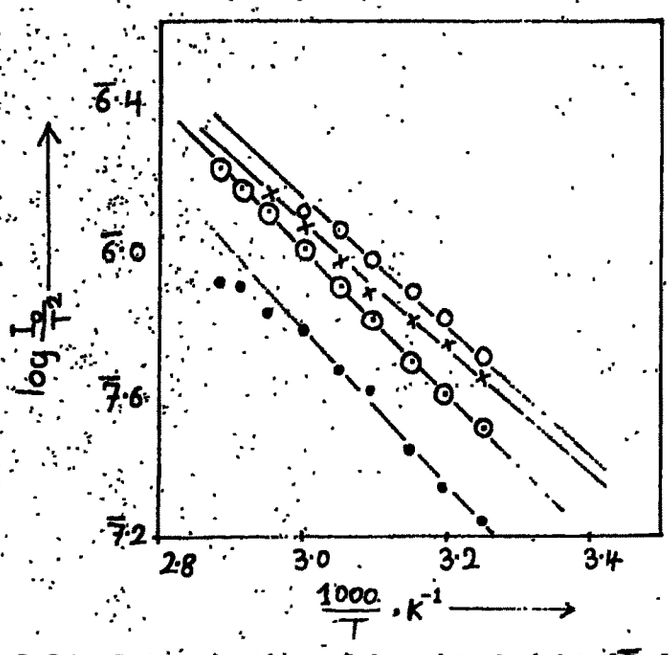

Fig.5.6 : Determination of barrier height [Φ_B] for various cell configuration :
1) ⊙ - pure CdS (2) O - 0.005 wt% CdS:Sb
3) ● - 0.075 Wt% CdS:Sb (4) x - 0.25 wt% CdS:Sb

[45,110].

The barrier height for different cell configurations have been determined by measuring the reverse saturation current at different temperature for a fixed applied voltage. For a Schottky barrier junction, the reverse saturation current I_o is related to the built in potential ϕ_B as

$$I = A^* T^2 \exp(-\phi_B / KT) \qquad \ldots (5.6)$$

where A^* is Richardson's constant and ϕ_B is the barrier height at equilibrium. The energy level diagram for both semiconductor-metal and semiconductor-electrolyte junctions are identical to each other and hence equation of S-M junction have been applied to S-E junction by many workers [111,112].

The reverse saturation current is observed to vary exponentially with temperature. The variation of $\log (I_o/T^2)$ vs $1/T$ for three typical cells is shown in fig. 5.6. The slope of this plot gives built-in potential (ϕ_B).

b) Capacitance-Voltage characteristics in dark :

The electrode/electrolyte interface can further be analysed to obtain the flat band potential by the measurement of a space charge capacitance. It gives a correlation between charge density and electrostatic potential. Since the electrostatic potential cannot be measured directly the most valuable information can be

obtained from the capacitance measurement of a space charge layer. Thus the measurement of differential space charge layer capacitance provides a convenient tool for obtaining the useful informations about both the semiconductor and an electrolyte. For the semiconductor electrolyte solar cells, the obsserved capacitance corresponds to the semiconductor depletion layer, since the capacitances due to Helmholtz and Gouy diffused layers are assumed negligible due to high ionic concentration of an electrolyte. The capacitance is related to voltage as [45,113].

$$C^{-2} = \frac{2}{q \epsilon_s \epsilon_o N_D}\left[V - V_{fb} - \frac{KT}{q} \right] \qquad \ldots (5.7)$$

where, ϵ_s is a dielectric constant of a semiconductor, ϵ_o is permittivity of the free space, N_D is the carrier density and V is the applied voltage, V_{fb} is the flat band pontential.

The measurement of capacitance vs electrode potential (vs SCE) was performed as explained in the above section. The capacitance is found decreased with increased electrode potential. The Mott-Schottky plots are constructed from these observations and are shown in fig. 5,7. It has been found that the variation of C^{-2} vs V (SCE) deviates from the linear behaviour at high applied reverse voltages. The non-linearity is an indicative of the graded type of junction [45,67,114]. The departure from an ideal behaviour has been caused by non-uniform d.c. current distribution (owing to an edge

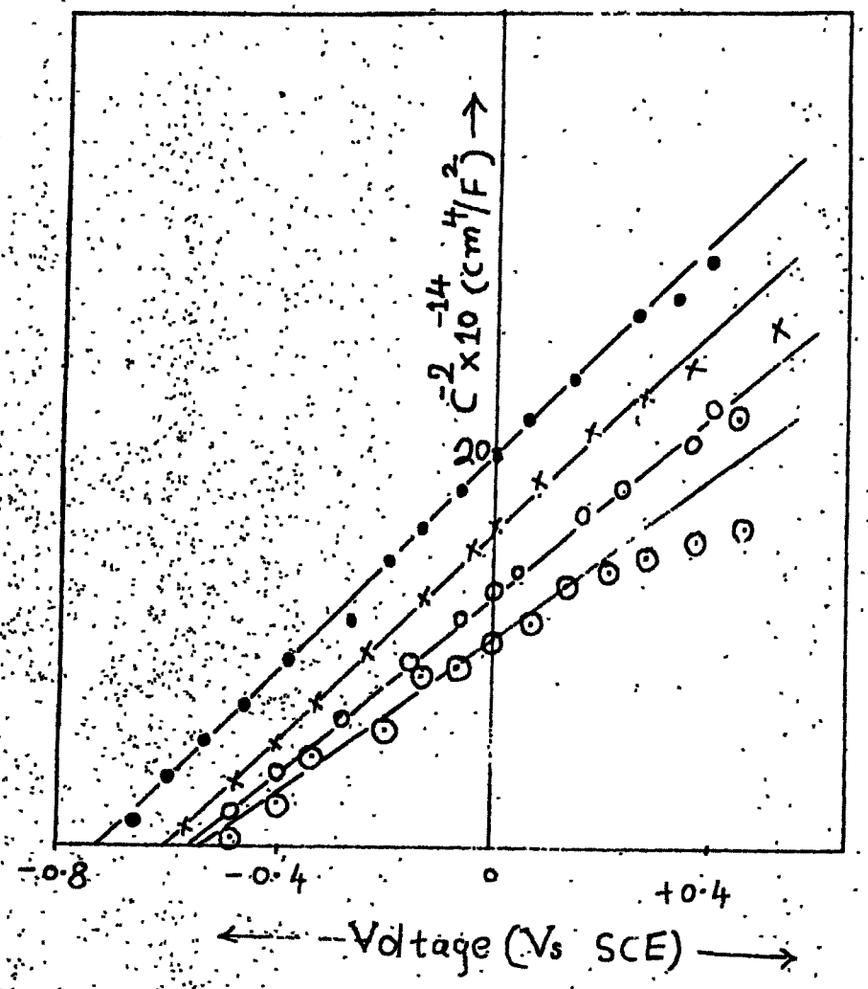

Fig. 5.7 : Mott-Schottky plots for four typical cells formed with Photoelectrodes :
1] ⊙ - pure CdS (2) O - 0.01 wt% CdS:Sb
3) ● - 0.075 wt% CdS:Sb (4) x - 0.1wt% CdS:Sb

effect, non planar interface, surface roughness etc). the presence of both types of impurities, ionic absorption on the surface of the semiconductor material and partly to the surface states [67,114]. Extrapolation of C^{-2} vs V plot to the voltage axis gives the magnitude of the flat band potential, V_{fb}. Various V_{fb}'s are listed in table 5.1. Since the V_{fb} is a measure of potential which must be applied to the semiconductor such that the bands remain flat at the interface, the V_{fb} determines the amount of band bending.

c) Current voltage characteristics in light :

The photovoltaic power output curves were recorded under 100 mW/cm^2 by means of a variable D.C. power supply and are shown in fig. 5.8. When a PEC cell is irradiated, the current voltage characteristic shifts in fourth quadrant thus indicating a generator of an electricity which is in accordance with the standard principles of the PEC cells [115]. It has been found that under unbiased condition the photoelectrode becomes more and more negative upon illumination showing that the material is n-type [116]. This is in accordance with the observations on thermoelectric power. The generation of a photovoltage and a photocurrent property of a photoelectrochemical cell can be understood from the equivalent circuit of a cell. An equivalent circuit of a PEC cell is shown in fig. 5.9. The photocurrent is

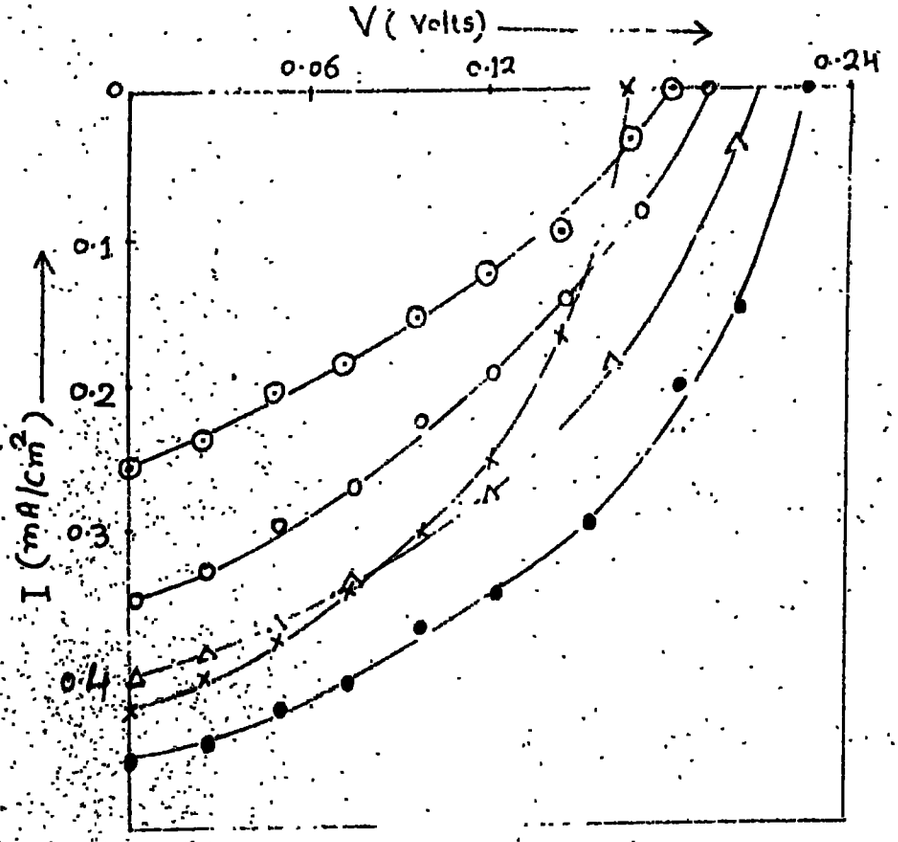

Fig. 5.8 : Photovoltaic power out put curves for five typical Cells :
1] ⊙ - pure CdS (2) O - 0.01 wt% CdS:Sb
3] Δ -0.05 wt% CdS:Sb (4) ● - 0.075 Wt% CdS:Sb and
5] x - 0.1 wt.% CdS:Sb

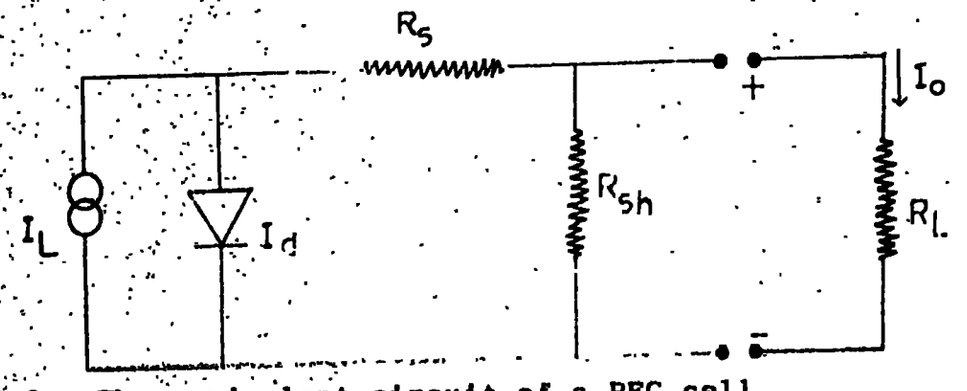

Fig. 5.9 : The equivalent circuit of a PEC cell.

represented by a current source. The forward current of a junction in dark is I_d, the series resistance of a cell is represented by a fixed lumped resistance, R_s which arises from the bulk resistance of a material [45,83]. The back contact of a cell is considered to be ohmic and the electrolyte offers a negligible resistance to the flow of current. The shunting effect through micro pores and along the edges of the photoelectrode is shown as R_{sh} [83]. R_L is the load resistance to the cell and V_{oc} is the open circuit voltage obtainable from a cell. We consider the Schottky diode equation for the S/E interface and thus the total current of a cell under illumination can be given as [12].

$$I = I_L - I_d - \frac{V_{oc}}{R_{sh}} = I_L - I_o\left[\exp\left(\frac{qV}{\eta_d KT} - 1\right)\right] - \frac{V_{oc}}{R_{sh}} \qquad \ldots (5.8)$$

where, I_L is the photocurrent, I_d is the dark current, I_o is the reverse saturation current and V is the applied voltagae. As R_{sh} for the cell is expected to be very high, V_{oc}/R_{sh} is meaningless and equation (5.8) takes the form asks

$$I = I_L - I_o\left[\exp\left(\frac{qV}{\eta_L KT}\right) - 1\right] \qquad \ldots (5.9)$$

For bias voltages exceeding $3KT/q$ one can also neglect last term in equation (5.9) Moreover, at open circuit condition $I_L = I_d$ and $V = V_{oc}$, thus rearrangement of equation yields to [12,45].

$$V_{oc} = \eta_L \frac{KT}{q} \ln \cdot \frac{I_{sc}}{I_o} \qquad \ldots (5.10)$$

At short circuit condition, $V_{oc} = 0$ and

$$I = I_L - I_o = I_{sc} \qquad \ldots(5.11)$$

The power output curves can be reporduced and the different cell parameters such as series resistance (R_s), shunt resistance (R_{sh}), fill factor (ff), and energy conversion efficiency (η) are computed and are listed in table 5.1.

5.3.2 Optical properties.

The three major optical features studied for all the cell structures are: photoresponse, spectral response and speed of response.

a) Photoresponse :

This is the dependence of short circuit current I_{sc} and open circuit voltage, V_{oc} on illumination light level, F_L. This is depicted in fig. 5.10. The photocurrent, I_L is found to have a direct bearing on F_L for low level of illumination and obeys the linear relation as [28].

$$I_L = C.F_L \qquad \ldots(5.12)$$

where C = constant of proportionality which depends on the fraction of light utilised for the generation of the number of carriers.

For higher excitation levels I_{sc} deviates a litle from linearity which can be ascribed to the series resistance effect.The photoelectrochemical reactions at the semiconductor-electrolyte interface can be observed if

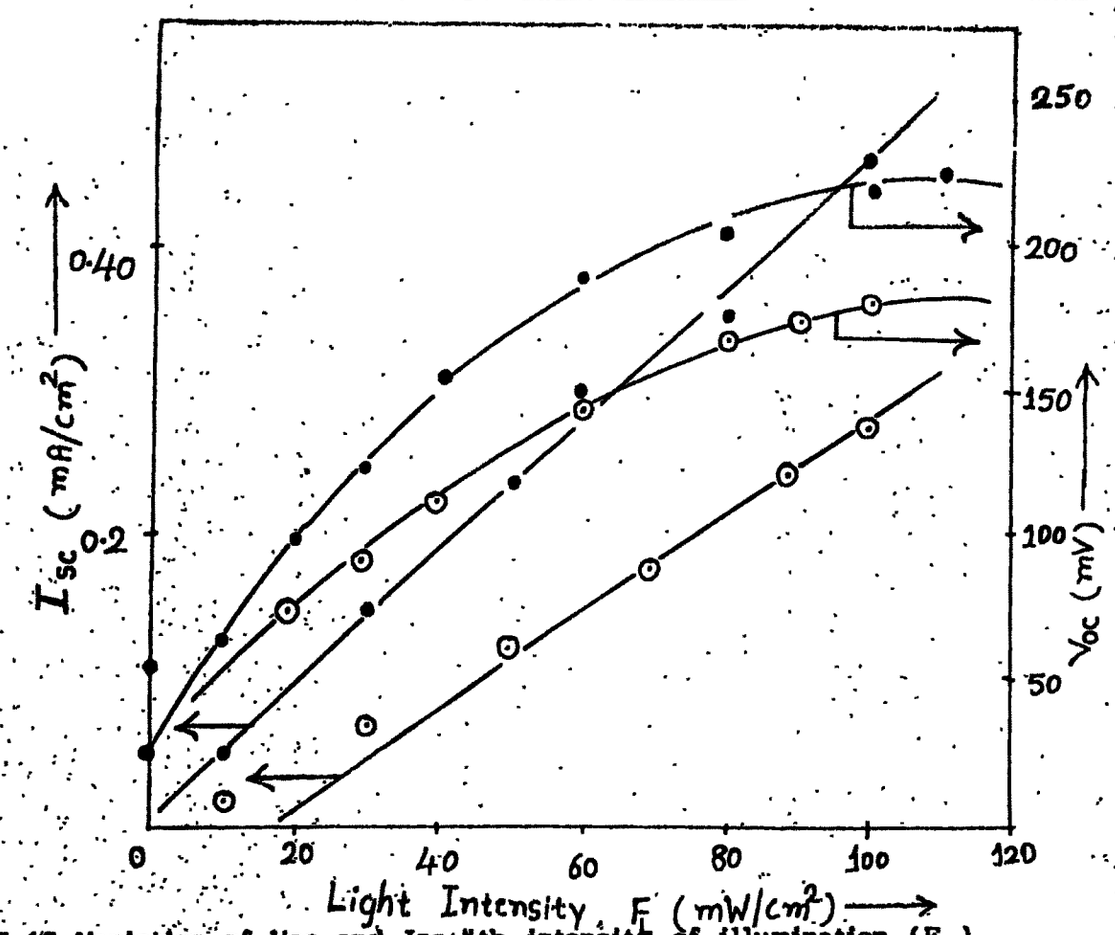

Fig.5.10 Variation of Voc and Isc with intensity of illumination (F_L) (1) ⊙ - pure CdS and (2) ● - 0.075wt % CdS:Sb.

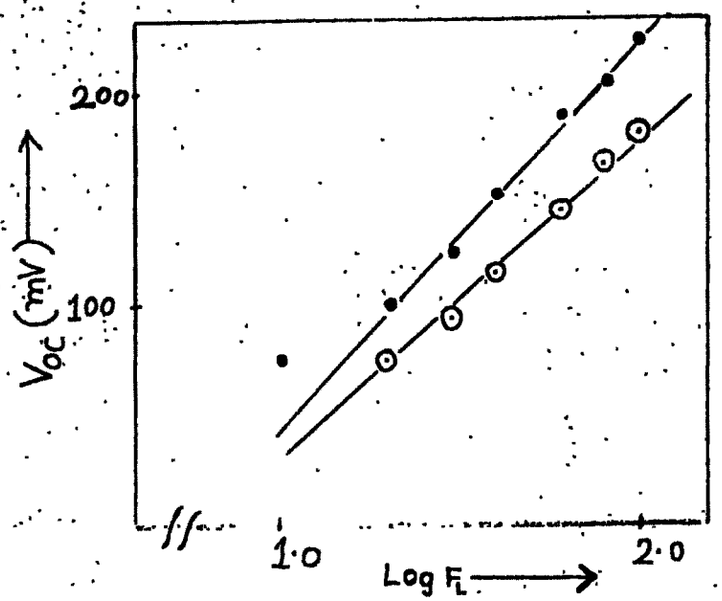

Fig.5.11 Determination of lighted quality factor(nL) of PEC junction with 1] ⊙ - pure CdS and (2) ● -0.0 75 wt% CdS:Sb, as the photoelectrodes.

minority carriers are generated by light absorption and finally they can reach the photoelectrode surface during their life time. The net current is therefore, dependent on various competing processes. The externally measurable current therefore, is a difference between the actual photocurrent and the forward current of the majority carriers. If the later is decreased to zero only photocurrent can be observed as :

$$I_{ph} = I - I_{redox} \qquad \ldots (5.13)$$

where, I = observed total current and I_{redox} current due to oxidation - reduction with surface states. In the absence of surface recombination and fast rate of electron transfer, the photocurrent increases steeply with F_L [117].

The variation of V_{oc} with F_L shows (fig. 5.10) saturation at high light levels which clearly indicates that V_{oc} depends upon the extent of band bending and change in the photo-fermilevel of the photoelectrode [117]. For an ideal photovoltaic device the dependence of V_{oc} should follow equation (5.10), which defines the movement of Fermi level in the bulk with increasing light intensity. In this case the surface states act as recombination centres [117] which cause to saturate the open circuit voltage resulting into low fill factor (ff) and efficiency (η) [118]. The photoresponse spectra is further analysed to determine the lighted quality factor of an illuminated junction. The plots of V_{oc} vs. ln F_L

are shown in fig. 5.11 for $I_0 <<< I_{sc}$. The magnitudes of n_L can be determined from the slope of these plots and are slightly smaller than their n_d's. This is in accordance with the results reported by Deshmukh et.al [45].

b) Spectral response :

The spectral response is an important technique utilised for the determination of the mode of transition of the semiconductor. There are some other techniques to determine this mode of transition, such as photoconductivity, reflectance, photoemission, intrinsic conductivity, optical absorption, and electroreflectance, however these are tedious than that of the spectral response. The response involves the measurement of short circuit current with wavelength. This is shown in fig. 5.12 for three PEC cells. Before the measurement, the dark current of a cell has been nullified by using a potentiometric arrangement as shown in the fig. 5.13. The cell was mounted on a spectrophotometer and shsort circuit current was measured for various wavelengths ranging from 400nm to 1000 nm. It is observed from the response that the photocurrent decreased both for shorter as well as longer wavelengths. Photocurrent decay on longer wavelength side is attributed to the non-optimised thickness and transition between defect levels [119]. The decrease in current on shorter wavelength side is due to the absorption of light into

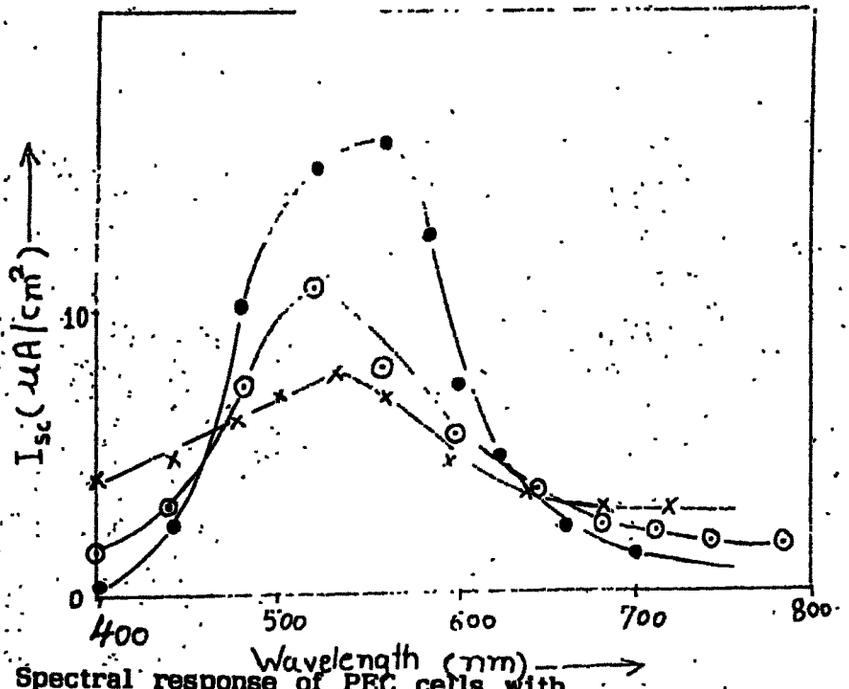

Fig. 5.12 : Spectral response of PEC cells with
1) ⊙ - undoped CdS (2) ● - 0.075 Wt% CdS:Sb and
3) x - 0.25 wt.% CdS:Sb, photoelectrodes.

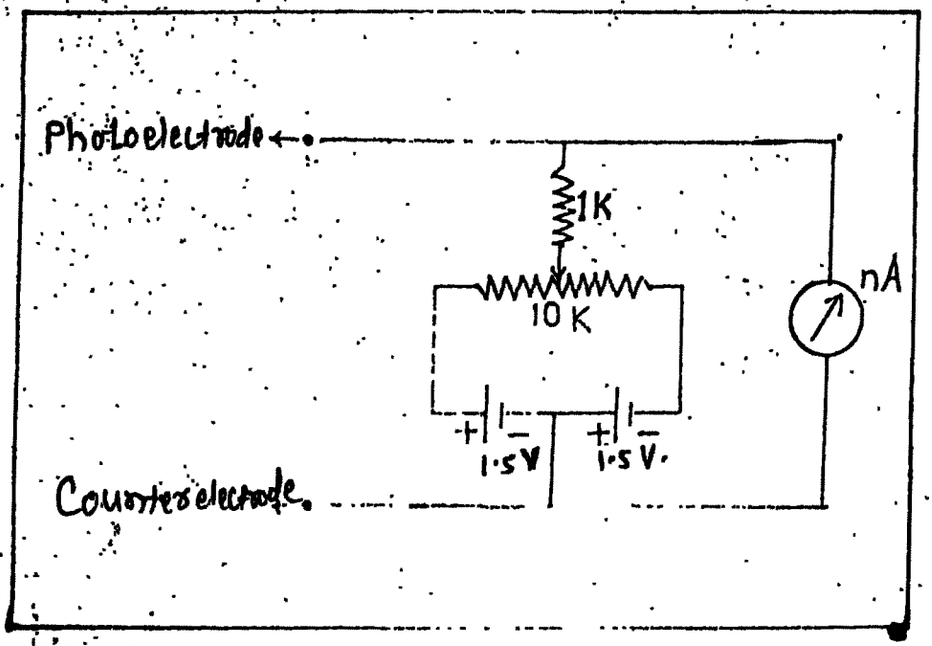

Fig. 5.13 : An arrangement for nullifying the dark current of a cell while measuring a spectral response.

an electrolyte and presence of surface recombination centres and to damages or impurities in the bulk very near the surface [119]. Thus spectral response gives a remarkable conclusion regarding the impedement of the hole transfer across the semiconductor/electrolyte interface. The spectral response also gives an information regarding the optimal band gap of a material for an efficient absorption, the theoretical consideration being 1.4 eV. In addition to the optimal band gap it is desirable to use semiconductor with direct electronic transition mode. According to Gartner's model [120] one can analyse the photocurrent density, I_{ph} of a cell near the absorption edge as :

$$I_{ph} = \frac{C(h\upsilon - E_{ind})^2}{h\upsilon} \quad \text{(for indirect mode)} \quad .. \quad (5.14)$$

and

$$I_{ph} = \frac{C(h\upsilon - E_d)^{1/2}}{h\upsilon} \quad \text{(for direct mode)} \quad .. \quad (5.15)$$

We can expand I_{ph}^2 of equation (5.15) in the parameter $h\upsilon - E_d$ upto a linear term (in this case I_{ph}^2 is linear with $h\upsilon$) close to E_d and it vanished at $h\upsilon \cong E_d$. This is helpful for determining the band gap of the material under study.

c) Speed of response :

The speed of response characteristic of a PEC cell is the rise and decay of I_{sc} and V_{oc} with time. Time required for I_{sc} and V_{oc} to decay to its original value after removal of the light exication is known as decay time. In the present investigation V_{oc} decay is studied

in order to understand the charge transfer mechanism across the interface. Most of the role of charge transport is played by the ions in the electrolyte. V_{oc} decay for two typical configurations is shown in fig. 5.14. Relatively fast rise and slow decay is observed at 100 mW/cm^2 light intensity.

The decay of V_{oc} follows the relation of second order kinetics [24] as :

$$V_{oc}(t) = V_{oc}(0)\ t^{-b} \qquad \ldots (5.16)$$

where $V_{oc}(0)$ and $V_{oc}(t)$ are open circuit voltages at t=0 and at t seconds and b is the rate constant. Further slow decay in V_{oc} can be attributed to the presense of surfacae states and hence the Fermilevel pinning.

In conclusion, a photoelectrochemical cell formed with chemically deposited n-CdS shows a poor performance. The major reason is its high electrical resistivity and it should be decreased in order to extract an expected power output. Attempts are now in progress to optimse the material in various views such as thickness of the photoelctrode, series diode type of cell configuration etc.

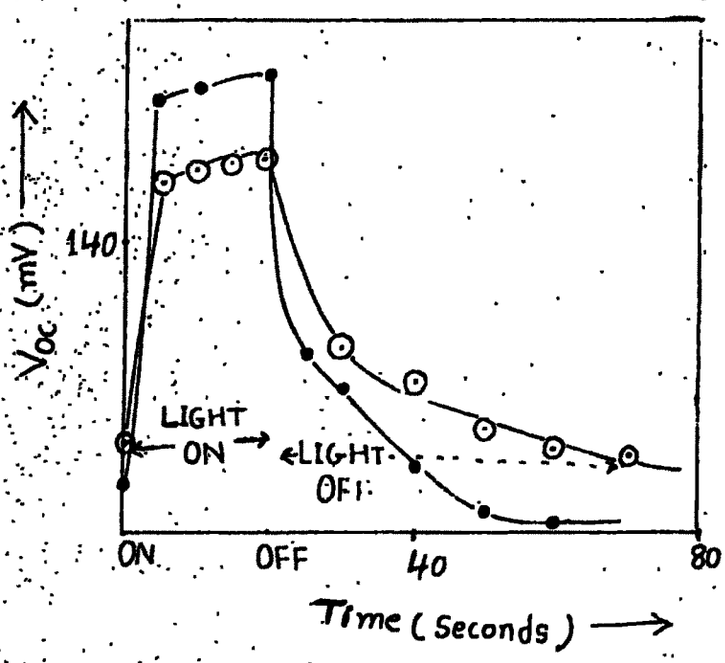

Fig. 5.14 : Variation of open circuit voltage Voc with time
1] O - as deposited CdS and
2] ● - 0.075 wt % CdS:Sb

Table 5.1

Computation of the performance parameters of a PEC cell for various compositions of CdS : Sb electrodes.

Sr. No.	Cell formed with photoelectrode composition	I_{sc} (mA/cm^2)	V_{oc} (mV)	R_s (Ω)	R_{sh} (Ω)	ff %	η %	n_d	n_L	V_{fb} volt
1	Pure CdS	0.255	180	436	1.333	31.3	0.014	2.61	2.60	-0.5
2	0.005 wt% CdS:Sb	0.290	184	-	-	-	-	2.72	2.60	-
3	0.01 wt% CdS:Sb	0.345	190	377	1.307	41.2	0.022	2.32	2.64	-0.5
4	0.025 wt% CdS:Sb	0.365	197	-	-	-	-	-	-	-
5	0.05 wt% CdS:Sb	0.400	205	300	1.600	40.8	0.033	2.24	-	-0.6
6	0.075 wt% CdS:Sb	0.460	220	192	1.714	45.4	0.046	2.17	2.97	-0.7
7	0.1 wt% CdS:Sb	0.420	172	200	0.960	42.2	0.031	2.39	-	-0.6
8	0.25 wt% CdS:Sb	0.180	160	470	0.830	-	-	2.81	2.23	-